J. Umm Al-Qura Univ. Eng.Archit.
https://doi.org/10.1007/s43995-023-00045-x

ORIGINAL ARTICLE

Validation of numerical results of complex seismic analysis through simple analytics

Giuseppe Brandonisio[1] · **Muhammad Tayyab Naqash**[2]

Received: 23 October 2023 / Accepted: 9 December 2023

Abstract
The paper analyzes the application of the numerical findings of the program, which is becoming increasingly difficult for civil and structural design. Since, as in many other countries, the verification of design using a software model is now required by current Italian codes as well. Given this, the structural engineer must provide a technical report using a licensed software tool, attached to other project documents to get the Seismic Authorization at the local Civil Engineering Department offices. Following a brief explanation of structural analysis methodologies, this study presents a criterion for assessing the applicability of numerical findings obtained using any structural software. Three case studies of this criterion are shown to demonstrate how to check them using simple manual calculations: (i) the normal stress in RC columns subjected to gravity loads; (ii) the periods of vibration, participating masses, and seismic base shear derived from dynamic modal analysis; and (iii) the main parameters characterizing the pushover curves of existing buildings. Finally, this work underlines the significance of confirming the application of numerical results obtained by software in civil and structural design. The offered criteria and scenarios exhibit realistic techniques to ensure accuracy and reliability in structural performance assessment, according to the structural requirements imposed by current codes in Italy and similar countries.

Keywords Seismic analysis · Structural design · Numerical validation · Software application · Structural performance assessment · Civil engineering codes

1 Introduction

The current Italian Technical Standards for Construction (NTC2018) [1] confirm what the previous version (NTC2008) [2] had prescribed about the applicability of numerical findings acquired by structural software. The Italian building code requires the structural designer to report the results of the elaborations to certify their trustworthiness. This evaluation will be compared to the outcomes of simple, even comprehensive, calculations performed on known schemes or solutions used, for example, in the structure's first proportioning phase. Furthermore, it will assess the consistency of the choices made in the schematization and modelling of the structure and activities based on considerations of the determined stress and deformation states. According to the Italian building code, the analysis, such as the equilibrium between constraint reactions and applied loads and comparisons between the analysis results and simplified evaluations, must be briefly illustrated in the report [3]. Consequently, for over a decade, the designer/structural technicians learned to produce an additional technical document, generally not exceeding a page, attached to the design report delivered to the Civil Engineers. Without the design report, the Civil Engineering Department's local offices do not authorize the project [4–6].

Checking the structural calculation quality carried out with the software aid is justified by analysing the results with the input parameters (geometric, mechanical, and loads) and increasing their complexity. Pushover linear analysis is now a standard tool, especially for assessing the seismic vulnerability of existing structures. To this end, we can recall the words that Lourenço quoted in his doctoral thesis: "The

✉ Muhammad Tayyab Naqash
engr.tayyabnaqash@gmail.com; mnaqash@iu.edu.sa

Giuseppe Brandonisio
giuseppe.brandonisio@unina.it

[1] Department of Structures for Engineering and Architecture, University of Naples Federico II, Naples, Italy

[2] Civil Engineering Department, Faculty of Engineering, Islamic University of Madinah, Prince Naif Ibn Abdulaziz, Al Jamiah, Medina 42351, Kingdom of Saudi Arabia

Published online: 16 January 2024

solution of a non-linear problem does not necessarily exist, and when it exists, it is not necessarily unique" (Lourenço, 1996) [7].

For "Smart Structural Designers," this check must be carried out (or, instead, it has always been done) regardless of the mandatory code. It should be noted that the work of the "Smart Structural Designer" is becoming more widespread and can quickly "satisfy this regulatory imposition," even with the same method used to run the numerical analysis, using the same software to check the reliability of results." "Between the "good and conscientious structural engineer" and the "smart structural engineer," there is a third category of professionals, which can be defined as the "quasi-smart structural engineer." It complies with the obligation of calculation imposed by the standard, such as extracting a floor joist from a complex building with the load acting on it. It is known as a "quasi-smart" and performs load analysis of structures. Consequently, the "quasi-smart structural engineer" compares the value of the maximum bending moment given by the tool (e.g., 114.5 kN m) from $qL^2/8$ of a simply supported beam (e.g., 125 kN m), concluding that since 114.5 kN m and 125 kN m have the same order of magnitude, therefore the results of a whole complex building are reliable [8].

With this article, we would like to provide examples of simple manual calculations to check various structural finite element analyses with increasing complexity. This work aims to show how it can comply with the standard's obligation using the tools acquired during several structural engineering checks, such as the column's plastic hinge translation at the base [9–11].

2 Seismic analyses of structures

What distinguishes the structural engineer from other professionals involved in the construction and infrastructure field is structural analysis. Structural analysis can be likened to the crystal ball of clairvoyants when using a metaphor. It allows us to understand the present condition of the structure. Also, it helps us to predict what will happen to the structure in the future under the acting actions, stresses, and deformations. In consulting this tool, the structural engineer also has the task of formulating a judgment on safety, obviously valid for the present and future during the structure's service life.

In contrast to the astrologer, the structural designer draws on structural mechanics theory developed over millennia by structural mechanics scholars. This information may be traced back to Galileo's pioneering investigations in 1638, which investigated material resistance and developed the constitutive law of elasticity. From Hook's work in 1678 to the reviews on Euler–Bernoulli deformations in the eighteenth century. Since the invention of the Navier beam theory in 1826, a series of structural analysis methods have evolved over the years [12]. These techniques have emerged to investigate the behaviour of elastic structures under both static and dynamic situations. The technical literature has presented several structural computation methods, encompassing approaches for assessing forces and deformations as calculating tools have evolved [13–15].

Together with the methods of analysis of elastic structures, the trend of the plastic calculation of structures has also spread in the last century, with the studies of Kazinczy (1914) [16] on steel beams, Baker (1949) on steel frames [17], Onat and Prager (1952) on steel arches [18], Kooharian (1952) on concrete segment arches [19], with the most recent studies by Heyman (1966) given the formulation of the three general hypotheses for the application of limit analysis to structures in masonry [20, 21].

After this brief historical overview, we would like to highlight how many studies conducted in the past centuries have been somehow captured by the crystal ball used by today's structural engineers and influence daily professional activities. To this end, the beam theory, used to develop the member's stiffness matrix according to its geometry, is assembled by the FEM calculation software in the entire structure's stiffness matrix. Furthermore, it is enough to think that starting from Kazinczy and Baker, we have arrived at today's concepts of classification of steel sections of §4.2.4.1 of the NTC2018 for collapse mechanisms, used to consider for the capacity design criterion implemented in §7 of the NTC2018. The same hypotheses proposed by Heyman for the limit analysis of masonry arches can be found in §8.7.1 of the current technical standards for the seismic analysis of local mechanisms.

Concerning the calculation of structures subjected to seismic actions, chapter 7 of the NTC2018 specifies that the analysis can be linear or non-linear (Fig. 1) and classified into static or dynamic with the fact that the balance between the actions and the reactions of the structure both treated in the static or dynamic field, respectively. Therefore, the seismic analysis of structures can be conducted using one or more of the following methods, listed by increasing levels of complexity:

Structural engineers use the linear static analysis for the seismic design up to NTC2008 and consists of applying the static forces equivalent to the inertial actions induced by the earthquake. It represents a simplification of the linear dynamic analysis method since it assumes that the response of the structure to the earthquake can be well represented by the first mode of vibration alone, which is assumed to be linear, with an approximate vibration period that can be calculated as a function of height H of the building, i.e., the displacement d of the highest point of the building due to horizontal forces of the plane F_i of an entity equal to the respective seismic weights W_i. The mass participating in this

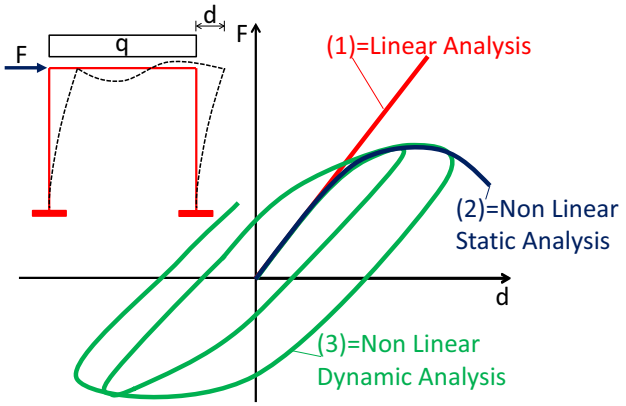

Fig. 1 Methods of seismic analysis

first simplified model is assumed to be proportional to the seismic weight W_{tot} of the entire structure for buildings up to two floors. A significant participating mass equal to 85% of W_{tot}/g is considered for buildings with at least three horizontals. Therefore, with this effective mass, it is possible to evaluate the inertial actions using the design response spectrum. For these simplifying hypotheses on the structure's dynamic properties to be satisfied, the construction must be regular, as it has a simple and predictable seismic response. According to NTC2018, the regularity of the construction response can be defined by measuring the regularity in plan and height, as indicated in §7.2.1. According to current legislation (§7.3.3. 2), it is possible to use linear static analysis only in the presence of regular buildings and a height that does not exceed 40 m. Therefore, the NTC2018 does not force the applicability of this method on the in-plan regularities. In any case, since this method belongs to the structural designer's due to its simplicity and familiarity with the topics covered in the Science and Technique of Constructions courses, therefore as a limitation it is advisable to use linear static analysis regardless of whether the regularity requirements are met. In the current case the manual method does not consider the infill walls, and these are also usually not considered in the modelling as well in the cases under considerations. Nevertheless, it is useful to consider them in the future studies to see their effect on the overall behaviour of the structure through numerical analysis as well through this simplified method. In elevation, it represents a valuable tool for checking the other analysis results described in the following section, which are gradually more complex and challenging to manage [22, 23].

2.1 Dynamic linear analysis

Dynamic linear analysis, or modal analysis with response spectrum, is the reference method for the seismic analysis of structures. Under the hypothesis of linear elasticity assumed for the construction's behaviour, differential equations that govern the dynamic equilibrium of the actions acting during seismic motion are transformed into many independent differential equations. Therefore, the structure's global response can be studied through the linear combination of the individual vibration modes that characterize each structure as a function of the lateral stiffnesses, the floor's seismic masses, and the structure's damping properties. As well summarised in §7.3.3.1 of the NTC2018, the linear dynamic analysis is divided into the following steps:

(i) Determination of the structure's modes of vibration, characterized by the modal forms ψ_i, by the participated masses M_i and the vibration periods T_i, indicated with the subscript i shows *the i-th* mode of vibrating the structure.
(ii) Evaluation of the effects of the seismic action, induced by the pseudo acceleration read on the design response spectrum in correspondence with each vibration period of the identified modes.
(iii) Combination of the effects induced by the seismic action for each mode, using the complete quadratic combination rule (CQC) which has definitively replaced the previous, more comfortable to apply SRSS rule. All vibration modes with participant mass greater than 5% and effective participant mass greater than 85% of the total mass must be considered for each analysed direction.

2.2 Modal analysis

Modal analysis with response spectrum is an evolution of the linear elastic analysis method, which also considers the effects of vibration modes higher than the first, thus considering irregularities in the building's dynamic response. Therefore, this type of analysis can also be used for irregular structures in plan and elevation. The critical aspect of linear dynamic analysis consists of the operational difficulty of determining structures' dynamic properties without using automatic calculation software and combining the effects with rules that are not intuitive from a physical point of view. It should be noted that both the rules for combining the SRSS and CQC effects were proposed by E. Wilson et al. in 1962 and 1988, respectively [24]. Nevertheless, in a recent publication, he expressed serious doubts about using this analysis method with modern calculation tools, manifesting it as a "structural coming out." He described it with the following sentences, leaving little space for interpretation: "*Ray Clough and I regret we created the approximate Response Spectrum Method (RSM) for seismic analysis of structures in 1962. After working with the RSM for over 50 years, I recommend it not be used for seismic analysis. The use of the Response Spectrum Method in Earthquake Engineering*

must be terminated. It is not a dynamic analysis method—The results are not a function of time (Wilson, 2015)" [25].

2.3 Static non-linear analysis

Static non-linear analysis, also called pushover analysis, is a simplified method that allows the development of the capacity curve of the structure, which is related to the base shear *Fb* and displacement *dc* of a control point, which for buildings is conventionally identified with the centre of gravity of the last floor of the building (see curve 2 of Fig. 1). The most widespread modelling criterion is that of concentrated plasticity. The model's non-linearities are localized at the ends of the beam elements through generalized force–displacement (e.g., moment–curvature) generally of an elastoplastic link. The capacity curve describes the evolution of the structure's response as the intensity of the horizontal plane forces increases, schematizing the earthquake's effect on the building. The intensity of the horizontal forces is made to grow monotonously until the collapse of the structure. According to §7.3.4.2, at least two distributions of inertial forces must be considered, the first related to the shape of the main vibration mode in the direction considered (which requires the need to carry out a preliminary modal analysis of the structure), the second distribution of the forces proportional to the seismic masses. The *Fb-dc* capacitance curves associated with the two force distributions in each direction are then transformed into the F^*–d^* curves of a structural system with a degree of freedom (S-DOF) equivalent to the structure under consideration (M-DOF). F^* and the displacements d^* of the equivalent S-DOF system are obtained from those of the M-DOF system by dividing the quantities F_b and d_c by the modal participation factor Γ. The capacitance curves F^*-d^* of the equivalent S-DOF system are then transformed into bilinear curves equivalent in energy terms, with equal areas subtended by the F*-d* curves and the corresponding bilinear ones. Once the bilinear capacitance curves of the S-DOF equivalent system have been constructed, the verification consists of determining in the ADRS (Acceleration–Displacement Response Spectrum) plane the displacement demand d_{max}^* (T^*) associated with the inelastic response spectrum and at period T^* of S-DOF system with the ultimate displacement d_u^* of the equivalent bilateral curve.

The strength of the static non-linear analysis method is undoubtedly identifiable in the possibility of visualizing the evolution of the structure's response as the horizontal forces increase, which helps understand global structural behaviour. However, it should be emphasized that most Structural Designers, especially the more seasoned ones, have little confidence in non-linear analysis methods. Also, in this case, it is considered useful to quote the words of Fajfar, who proposed the so-called N2 method which inspired the NTC2018: "*Despite the many simplifications which are involved in the N2 method and other pushover-based approaches, and despite many limitations which apply, these methods provide a lot of important information about the structural response. They should not be regarded as a replacement but rather a complement to standard elastic analysis as a second opinion*" (Fajfar et al., 2011, 2012) [26, 27].

2.4 Non-linear dynamic analysis

The non-linear dynamic analysis consists of modelling the effects of the seismic action using time histories of ground motion applied along with the structure's two main directions and, if necessary, in the vertical direction to consider the earthquake's vertical component. According to § 7.3.5 of the NTC2018, at least time histories must be adopted. Their effects on the structure must be evaluated as an average of the most unfavourable values. It is a type of advanced analysis for unconventional structures or structures requiring high seismic protection levels. Therefore, it requires in-depth knowledge of the structural engineer of modelling and analysis techniques in the non-linear dynamic field.

3 Acceptability of numerical results

Regardless of the structure's complexity under consideration and the analysis method used, it is essential to validate the automatic calculation results. Therefore, establishing an acceptability criterion valid for numerically measuring this is necessary. A possible criterion is proposed in Fig. 2, which shows a graph having the quantity deriving from the computational analysis to be controlled (for example, the bending moment of the centreline section of a beam, the normal stress at the base of a column, etc.) on the abscissa. The graph's ordinate axis shows the analogous control quantity deriving from the simplified analysis. The bisector OA of the chart represents points P. The two analysis methods, in comparison, return the exact result with a deviation equal to 0%. The pair of straight lines OB and OB* represents the locus of points characterized by differences between the magnitude deriving from the calculation and the simplified calculation equal to + 10% and − 10%.

Similarly, the pairs of lines OC and OC* are associated with ± 20% differences between the two quantities being compared. Therefore, the OBAB* is the Q points location characterized by differences between the quantities not exceeding the limit value of ± 10%, which has always been considered acceptable from an engineering perspective. Therefore, OBAB* can be defined as a "result acceptability zone."

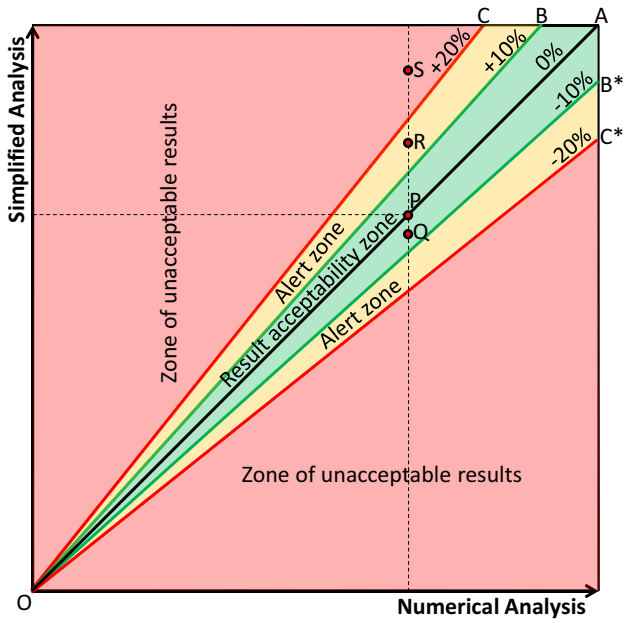

Fig. 2 Acceptability diagram for the results

The two zones, OCB, and OC*B*, represent R points characterized by differences in the obtained quantities between ± 10% and ± 20%; they can be called "alert zones for results." This means that the comparative quantities within these zones differ by a percentage and is unacceptable. Hence, it is necessary to understand these discrepancies, which may depend on the simplifications used for the analysis regarding the path of loads, static values adopted, and approximate values of the loads considered. Of course, if the percentage differences between the quantities being compared fall within the alert zone, it is essential to use the structural engineer's experience to understand whether these differences can be physically or numerically acceptable.

Finally, point "S", located above the line OC and below the line OC*, represents the computational results' non-acceptability. They are associated with deviations greater than ± 20%, except for gross errors on simplified calculations. Consequently, these areas of the graph have been called the "zone of unacceptable results."

In summary, if the point associated with the two quantities is to be compared arranged on the line OA as in point "P" in Fig. 2, we are in the "ideal case" of perfect equality between the resultants deriving from the two different analyses. Suppose the two comparative quantities are placed between OB and OB*, as in point Q in Fig. 2. In that case, the computational analysis results can be considered acceptable as they differ by no more than ± 10% compared to the simplified analysis. Suppose the comparison between the results gives rise to situations like those represented by point R in Fig. 2, located in one of the two alert zones. In that case, it is necessary to analyze both the hand and computational calculations in detail to understand the reason behind the disagreement, ranging between ± 10% and ± 20%.

Consequently, it is necessary to revise the simplified model to compare or modify the computational analysis's structural model. Finally, suppose the comparison gives rise to situations like those represented by point "S" in Fig. 2. In that case, it is undoubtedly necessary to review the computational model since the results are unacceptable; they differ by more than ± 20% from the results provided by the simplified analysis.

In the following, some examples of using the results obtained from the acceptability diagram will be provided to understand from a graphic point of view the usefulness of the measure of the deviation compared to the results obtained from the simplified analysis.

It is understood that the limits of ± 10% and ± 20% are assumed as threshold values between various zones in Fig. 2. These can be varied according to the complexity of the analysis being checked and the structural engineer's familiarity with the case under consideration.

4 Validation of computational results

In this section, some cases of simple hand calculations will be illustrated, helpful in checking the results deriving from the FEM numerical analysis of three case studies described for increasing levels of complexity. In fact, regarding both a simple two-story reinforced concrete building and a more complex seven-story one, we will illustrate some criteria that can be used to check the normal stress's acceptability in a column subjected to vertical loads only with linear and non-linear seismic analysis. Finally, a third example of checking the building results seismically isolated at the base will be shown.

Finally, it should be emphasized that FEM analysis can also be a useful control tool because the most straightforward and manageable linear static analysis can be used to verify the reliability of more complex linear dynamic and non-linear static analysis.

4.1 Case 1: two-storey R.C. building

The first application concerns the check on the calculations carried out for seismic retrofitting of an existing two-story reinforced concrete building built in the 1970s in Nola (NA), assumed to be a non-seismic area at the construction period. To this end, a three-dimensional structure model was created with the finite element program SAP2000 (CSI, 2018) [28], with static, linear, non-linear, and linear dynamic analyses.

Figure 3 shows the building under consideration, consisting of a portion made of masonry between 1920 and 1930s

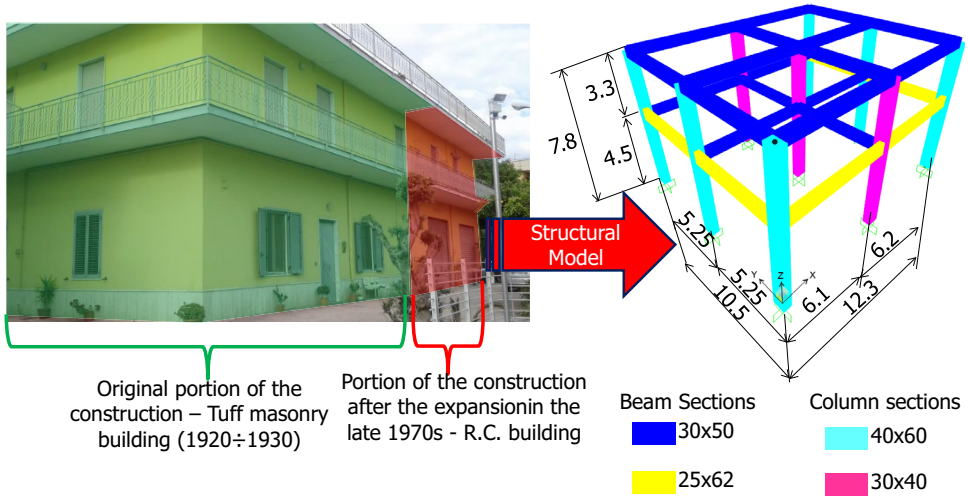

Fig. 3 Case 1: real building (left) identifies the reinforced concrete portion subject to seismic adaptation and the structure's finite element model (right)

(underlined in green). The remaining portion in reinforced concrete, highlighted in red was built to expand the building in the late 1970s. The right side of the figure shows the finite element model implemented in SAP2000. The figure also indicates the main global geometric dimensions and the cross-sections of beams and columns configuration (Marrazzo, 2020) [29]. The columns are composed of two different Sects. (40×60 and 30×40) whereas the beams are 30×50 and 25×62 as shown in Fig. 3. The Reinforce concrete materials composed of concrete of about *40* MPa and steel yield stress of about *320* MPa.

4.1.1 Verifications of normal stress in a column under gravity loads

The normal stress at the base of the central column obtained by the analysis conducted with SAP2000 under the vertical loads only combined with the Life Safety Limit State (SLV) is equal to Ncomp. = 644.5 kN, where the subscript "comp." means the quantity under consideration deriving from the computational analysis.

Considering that a typical building in reinforced concrete (Pagano, 1969) [30] at the SLV has a seismic weight (w) equal to about 10 kN/m^2 and that the tributary area of the column equal to (see Fig. 3):

$$A_{trib.} = 5.25 \cdot 6.15 = 32.29m^2 \tag{1}$$

An approximate value of the normal stress at the base of the column, neglecting the coefficients of continuity of the floor and beams, can be estimated using the following equation:

$$N_{simpl.} = n_{st} \cdot A_{trib.} \cdot w = 2 \cdot 32.29m^2 \cdot 10kN/m^2 = 645.80kN \tag{2}$$

The value calculated with Eq. (2) coincides with that calculated by the SAP2000, as shown in Fig. 4, which illustrates the acceptability diagram of this case's results. In fact, from Fig. 4, it is observed that the point associated with the two values of N compared is placed on the bisector OA of the diagram to confirm that the two methods of analysis in comparison yield practically the same result, confirming the agreement of the FEM modelling with SAP2000.

4.1.2 Control of modal dynamic analysis results

Once the FEM model's accuracy has been ascertained under vertical loads only, it is possible to carry out a higher level of control of the results deriving from the modal analysis conducted with the software calculations.

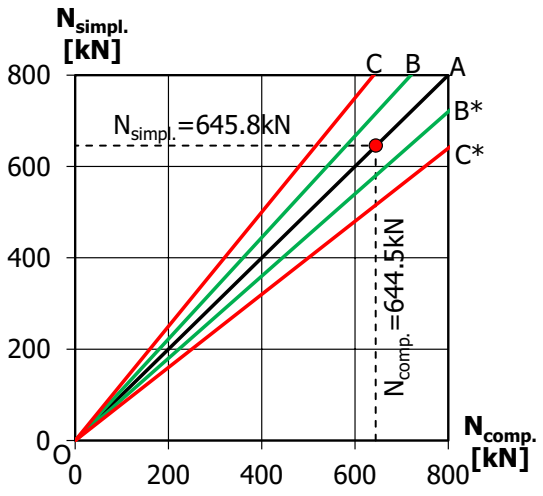

Fig. 4 Case 1: acceptability of results for normal stress at the central base column

For case study 1, the modal analysis was conducted with SAP2000, as shown in Fig. 3. It can be observed from Fig. 5 that the first vibration mode is a pure translation in the x-direction, with a period equal to $T_{comp.,x} = 0.42$ s, and participant mass fraction $M^*_{comp.,x} = 94\%$. The second mode of vibration, on the other hand, is translating type along the y-direction with slight rotation (4%); the corresponding period of vibration is $T_{comp.,y} = 0.38$ s, while the participating mass fraction is equal to $M^*_{comp.,y} = 90\%$.

The correctness of the vibration period results shown in Fig. 5 can be verified using the NTC2018 simplified formula [7.3.6] as given by Eq. 3:

$$T_1 = 2 \cdot \sqrt{d} \tag{3}$$

Being d the lateral elastic displacement, expressed in meters, of the highest point of the building deriving from the application of horizontal forces equal to the seismic weights of the floor.

For the building in question, the seismic floor masses are equal to $W_1 = 1822$ kN and $W_2 = 1480$ kN, which, applied in the centre of gravity of the two diaphragms, in the horizontal direction, give rise to the following displacements at the tip of the building: $d_x = 0.048$ m and $d_y = 0.038$ m. Therefore, Eq. (3) offers the subsequent simplified periods along with the two main directions of the building:

$$\begin{aligned} &\text{direzione x: } d_x = 0.048\text{m} \Rightarrow T_{Simpl.,x} = 2 \cdot \sqrt{d_x} = 2 \cdot \sqrt{0.048} = 0.44s \\ &\text{direzione y: } d_y = 0.038\text{m} \Rightarrow T_{Simpl.,y} = 2 \cdot \sqrt{d_y} = 2 \cdot \sqrt{0.038} = 0.39s \end{aligned} \tag{4}$$

The comparison between the two fundamental periods of SAP2000 and those calculated with the simplified expressions (4) is shown in the diagram of acceptability of the results of Fig. 6a. This highlights that both points fall within the acceptability zone since the differences between said periods are 4.8% in the x-direction and 2.6% in the y-direction, respectively.

Another check of the agreement of the results of the modal analysis can be carried out on the values of the participating masses obtained from the numerical program for the first two modes, which are equal to $M^*_{comp.,X} = 94\%$, and

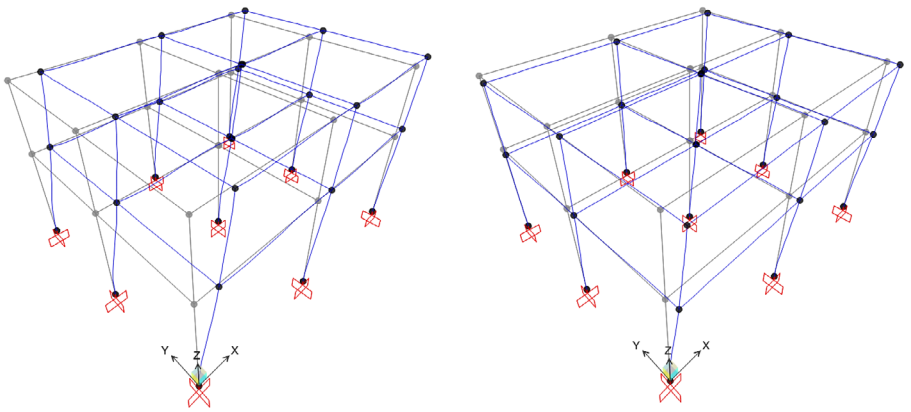

Fig. 5 Case 1: dynamic characteristics of the first two vibration modes of the structure

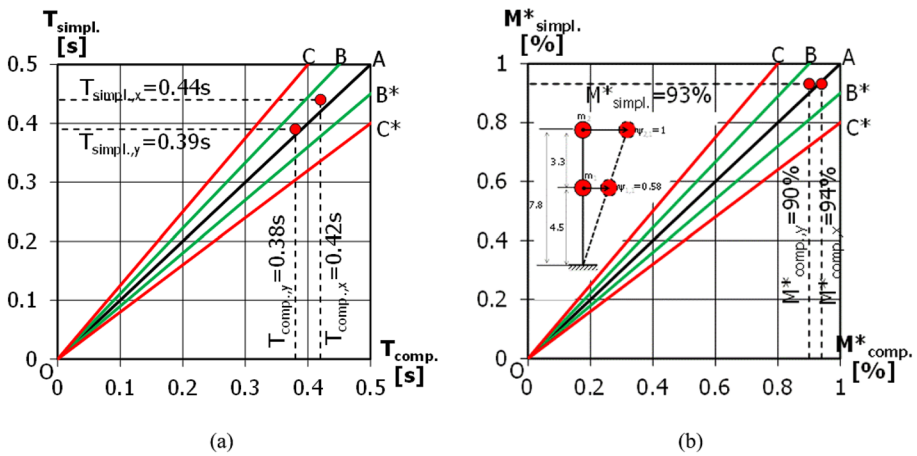

Fig. 6 Case 1: acceptability of the results regarding vibration periods (**a**) and participating masses (**b**)

$M^*_{comp.,\,Y} = 90\%$, respectively, as indicated in Fig. 5. To this end, considering the regularity of the structure in question, it is possible to hypothesize in a simplified way that the first modal is linear in both x and y-directions. Therefore, considering this simplified modal form normalized concerning the modal shift of the coverage ($\psi_{2,1} = 1$), we have (see the image in Fig. 6b):

$$\Psi_{1x,1y} = \left\{ \begin{matrix} \Psi_{2,1} \\ \Psi_{1,1} \end{matrix} \right\} = \left\{ \begin{matrix} h_{tot}/h_{tot} \\ h_1/h_{tot} \end{matrix} \right\} = \left\{ \begin{matrix} 7.8/7.8 \\ 4.5/7.8 \end{matrix} \right\} = \left\{ \begin{matrix} 1 \\ 0.58 \end{matrix} \right\} \tag{5}$$

Since the seismic masses of the two decks are valid:

$$m_1 = \frac{W_1}{g} = \frac{1821.93kN}{9.81m/s^2} = 185.75\frac{kN \cdot s^2}{m}; m_2 = \frac{W_2}{g} = \frac{1480.12kN}{9.81m/s^2} = 150.88\frac{kN \cdot s^2}{m} \tag{6}$$

The corresponding simplified participant mass percentage is:

$$M^*_{manuale} = \frac{\left(\sum_{j=1}^{2} m_j \cdot \psi_{j,1}\right)^2}{m_{tot} \cdot \left(\sum_{j=1}^{2} m_j \cdot \psi_{j,1}^2\right)} = \frac{\left(m_1 \cdot \psi_{1,1} + m_2 \cdot \psi_{2,1}\right)^2}{m_{tot} \cdot \left(m_1 \cdot \psi_{1,1}^2 + m_2 \cdot \psi_{2,1}^2\right)} = \frac{(185.75 \cdot 0.58 + 150.88 \cdot 1)^2}{336.63 \cdot \left(185.75 \cdot 0.58^2 + 150.88 \cdot 1^2\right)} = \tag{7}$$

$$= \frac{313.43}{336.63 \cdot 336.60} = 93.12\%$$

The comparison between the participating mass given by SAP2000 for the first two vibration modes and the one calculated manually with Eq. (7) is proposed in graphical form in the diagram of acceptability of the results in Fig. 6b. It can be observed that the two points associated with the masses calculated along the x and y directions are close to the bisector OA, with deviations of less than 3.5%.

The comparison in terms of periods of vibration and percentages of participating mass along the two main directions allows us to state that the FEM model also provides acceptable results for linear dynamic analysis. It further shows that there are no errors in the modelling as well during the assignment of the seismic masses to the structure phases.

4.1.3 Verifications of non-linear static analysis results

Since the calculations are related to seismic retrofitting of an existing reinforced concrete building, for case study 1, pushover analysis was also carried out to determine maximum accelerations that can resist before and after the retrofitting of the building. Figure 7a shows the capacity curves obtained using SAP2000 considering the distributions of the forces proportional to the masses applied in the x-direction on the FEM model. It is possible to observe that all the curves overlap and have an almost elastic trend up to the

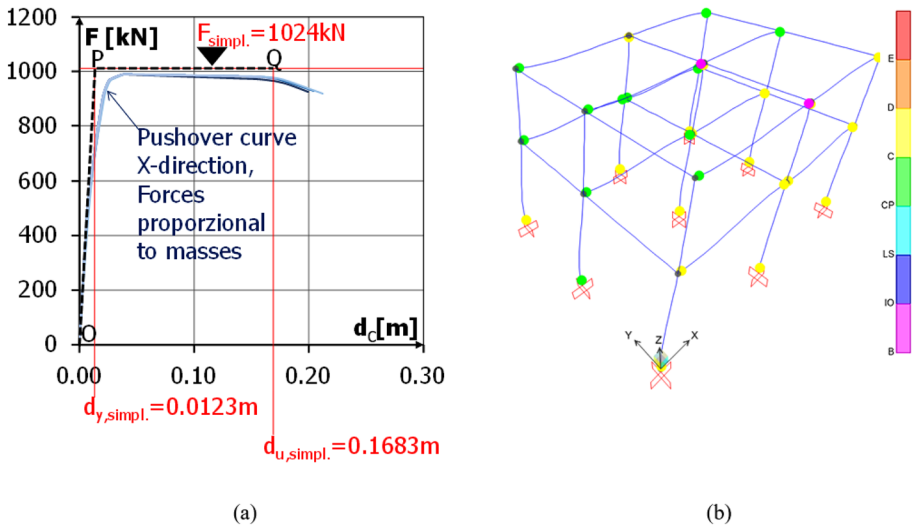

(a) (b)

Fig. 7 Case 1: **a** pushover curves at SAP2000 and comparison with manually calculated force and displacement values; **b** collapse mechanism of the structure analyzed at SAP2000

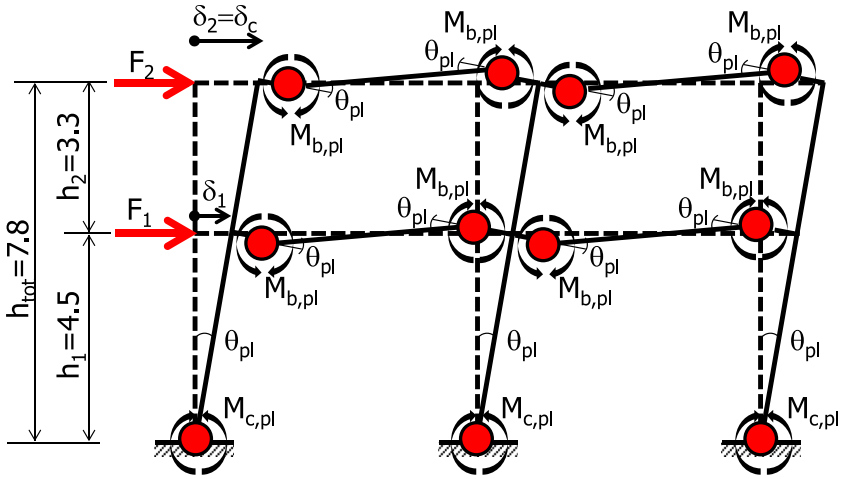

Fig. 8 Case 1: simplified global collapse mechanism

maximum base shear, equal to $F_{simpl.} = 990$ kN, also shows a plastic hinge with a slight reduction of resistances near the maximum displacement, equal to $d_{max,\,comp.} = 21$ cm.

Figure 7b shows the collapse mechanism of the structure given by SAP2000 in correspondence with the last step in the analysis. It is possible to observe the global collapse mechanism, characterized by flexural plastic hinges at the ends of all the beams and column bases of the first story.

The formation of this collapse mechanism suggests a control criterion for capacity curves based on applying the kinematic theorem of the limit analysis of structures (Massonet and Save, 1976) [31]. In fact, from the equality between the work L_e that the external forces F_1 and F_2 perform for the virtual displacements of the respective points δ_1 and δ_2 and the work of the internal forces L_i performed by the plastic moments M_{pl} of the hinges formed in the global mechanism of Fig. 8, we have:

$$\begin{aligned} L_i &= F_1 \cdot \delta_1 + F_2 \cdot \delta_2 = \left(F_1 \cdot h_1 + F_2 \cdot h_{tot}\right) \cdot \vartheta_{pl} \cong 2F \cdot \frac{\left(h_1 + h_{tot}\right)}{2} \cdot \vartheta_{pl} \\ L_e &= 2 \cdot n_b \cdot M_{b,pl} \cdot \vartheta_{pl} + n_c \cdot M_{c,pl} \cdot \vartheta_{pl} \\ L_i &= L_e \Rightarrow F_u = 2F = \frac{2 \cdot n_b \cdot M_{b,pl} + n_c \cdot M_{c,pl}}{\frac{\left(h_1 + h_{tot}\right)}{2}} \end{aligned} \tag{8}$$

kNm for all columns, the base shear that can withstand the structure collapse is:

$$\begin{aligned} F_{simpl.} &= \frac{2 \cdot n_b \cdot M_{b,pl} \cdot \vartheta_{pl} + n_c \cdot M_{c,pl} \cdot \vartheta_{pl}}{\frac{\left(h_1 + h_{tot}\right)}{2}} \\ &= \frac{2 \cdot 6 \cdot 150kNm + 9 \cdot 300kNm}{\frac{(4.3m + 7.8m)}{2}} = 1024.39kN \end{aligned} \tag{9}$$

This value is shown in Fig. 7a using the horizontal line passing through points P and Q.

Comparison between $F_{comp.} = 990$ kN and $F_{simpl.} = 1024.39$ kN is proposed in Fig. 9a. It can be observed that the corresponding point falls in the zone of acceptability of the results, being the difference between the two comparative quantities equal to 3.5%.

Comparisons were made on the displacements of the structure's control point to verify the capacity curves.

where: n_b is the number of beams at whose ends the plastic hinges of flexural strength $M_{b,\,pl}$ are activated; n_c is the number of columns at the base of which hinges are formed $M_{c,\,pl}$, while θ_{pl} is the plastic rotation, assumed in a simplified way the same for both beams and columns.

In the case in question, being $n_b = 6$ and $n_c = 9$, and assuming inconsistency with plastic hinges modelled in SAP2000, $M_{b,\,pl} = 150$ kNm for all beams and Mc, pl = 300

In fact, in a simplified way, it is possible to schematize the capacity curve through the bilateral OPQ, shown in Fig. 7a with the dashed line, where the points P and Q have been identified on the horizontal line corresponding to the resistance $F_{simpl.} = 1024.4$ kN calculated with the Eq. (9) corresponding to the displacements $d_{ysimpl.}$, and d_{usimpl}. They were calculated as reported in the following equation regarding the simplified global collapse mechanism of Fig. 8.

In particular, the displacement at elastic limit d_y was evaluated from the simplified formula [7.3.6] of the NTC2018 (see also Eq. (3)), noting that it derives from the

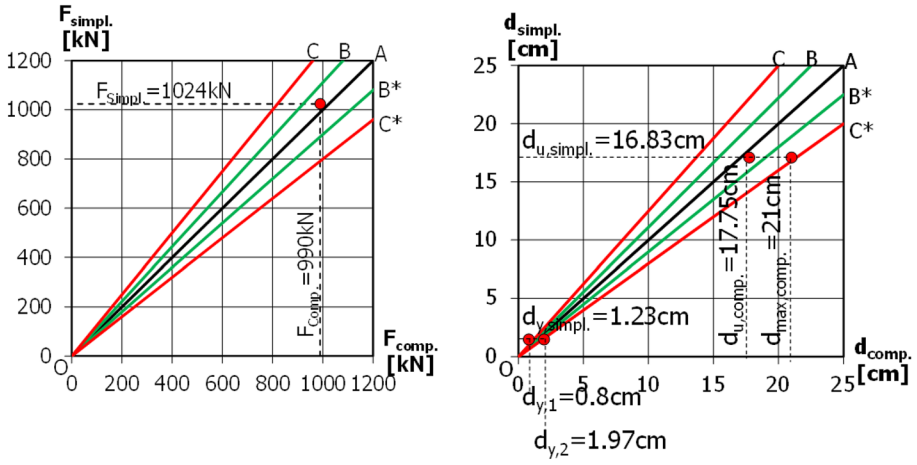

(a) (b)

Fig. 9 Case 1: acceptability of results regarding forces (**a**) and displacements (**b**)

simple period. Remembering that Eq. (3) d is the lateral elastic displacement of the highest point of the building deriving from the application of horizontal forces equal to the seismic weights of the floor, the following equality can be considered:

$$T_1 = 2\pi \cdot \sqrt{\frac{M_{tot}}{k}} = 2\pi \cdot \sqrt{\frac{W_{tot}}{g \cdot k}} = 2\pi \cdot \sqrt{\frac{k \cdot d}{g \cdot k}} \rightarrow W_{tot} = k \cdot d \tag{10}$$

therefore, as stated in §4.1.2. (dx = 0.048 m), the lateral stiffness k of the building in the x-direction can be estimated as:

$$k = \frac{W_{tot}}{d} = \frac{3300kN}{0.048m} = 68750kN/m \tag{11}$$

The displacement at elastic limit $d_{y,\,simpl.}$ Corresponding to the force $F_{simpl.}$ (point P) is:

$$d_{y,simpl.} = \frac{F_{simpl.}}{k} = \frac{1024.39kN}{68750kN/m} = 0.0149m \tag{12}$$

Consistently with the plastic hinge model implemented in the SAP2000 model, considering both for the beams and for the base of the columns, a rotational capacity equal to $\theta_{pl} = 2\%$ rad, the plastic displacement d_{pl} of the control point, equal to the PQ segment in Fig. 7a, can be estimated equal to (see Fig. 8):

$$d_{pl,simpl.} = \vartheta_{pl} \cdot h_{tot} = 0.02rad \cdot 7.80m = 0.156m \tag{13}$$

Therefore, the ultimate displacement of the control point can be calculated in a simplified way as:

$$d_{u,simpl.} = d_{y,simpl.} + d_{pl,simpl.} = 0.0124 + 0.156 = 0.1709m \tag{14}$$

The comparison between the values of the characteristic displacements of the pushover curves of Fig. 7a given by SAP2000 and those calculated by hand calculations through the simple Eqs. (12) ÷ (14) is shown in Fig. 9b, which allows observing that the displacements $d_{u,simpl.} = 0.1709$ m and $d_{u,simpl.} = 0.1757$ m are practically coincident, while $d_{u,simpl.}$ differs by less than 20% from the maximum displacement of the curve $d_{max,simpl.} = 0.1757$ m associated with the end of the degrading section of the pushover curves of Fig. 7a. Comparisons between the displacements at the elastic limit d_y can also be considered satisfactory, although they differ by about 20% due to the non-linearity of the pushover curves.

Finally, it should be noted that the values of $F_{simpl.}$, $d_{y,\,simpl.}$, and $d_{u,\,simpl.}$ allow tracing the OPQ curve with an elastic-perfectly plastic trend, which envelops the pushover curves well to confirm the correctness of the results obtained with the software and, simultaneously, the effectiveness of the simplified methods.

4.2 Case 2: seven-storey R.C. building

This paragraph illustrates cases to check calculations to assess the seismic vulnerability of an existing seven-story reinforced concrete building intended for residential purposes, built in 1963 in Gaeta (LT), an area not classified as seismic. This building was also analysed with a three-dimensional SAP2000 model (Fig. 10) through linear static analysis, linear dynamics, and non-linear static analysis. The floors are in brick with a height of 22 cm, and all the beams have a 25 × 65 section, except for the beams of the stairwell's intermediate landings (25 × 40) and two beams around the lift hole (25 × 50).

The building, being constructed at the start of the design and construction era, has frames only in the longitudinal direction (y), with the only exception of the transverse alignments in correspondence with the stairwell and the perimeter areas of the building, which have beams with a 25 × 65 section in the x-direction. The columns

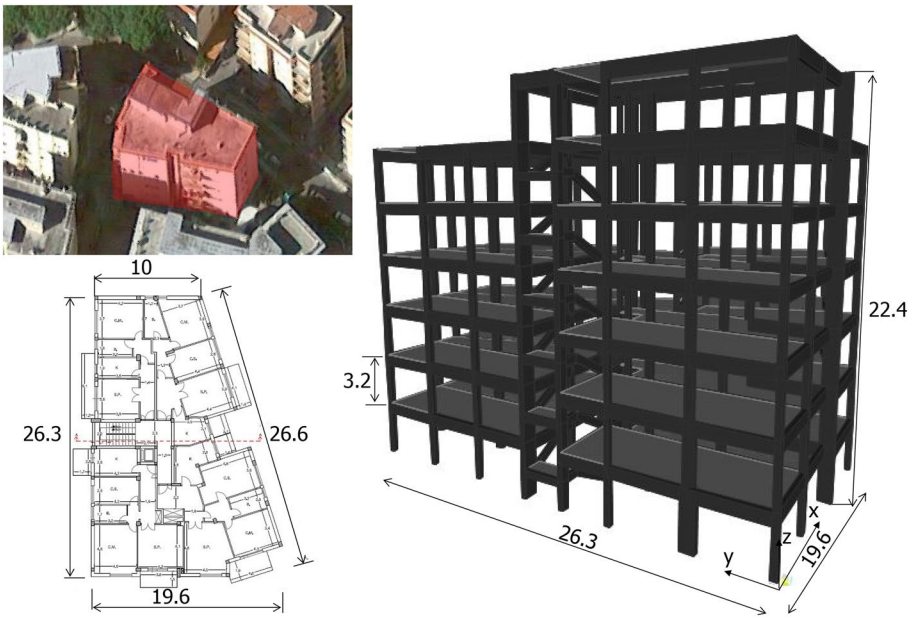

Fig. 10 Case 2: plan of the building, typical plan, and finite element model of the structure

are composed of five different sections (25 × 25, 30 × 30, 30 × 45, 30 × 50, 30 × 80) depending on their area of competence. The Reinforce concrete materials were characterized through a survey, which resulted in an average cylindrical resistance for concrete of about 40 MPa. The results of the tensile tests on the reinforcing bars showed an average value of the steel yield stress of about *320* MPa (Scipione, 2017).[32].

4.2.1 Verifications of normal stresses

For the vertical loads combined with the SLV, the SAP2000 analysis showed normal stress at the base of one of the central columns placed near the short side equal to $N_{comp.} = 1184.8$ kN.

The tributary area of the column is equal to $A_{trib.} = 18.55$ m^2. As stated in § 4.11, considering an approximate seismic unit weight w = 10kN/m^2, the approximate value of the normal stress at the base of the column is:

$$N_{simpl.} = n_{st} \cdot A_{trib.} \cdot w = 6 \cdot 18.55 m^2 \cdot 10 kN/m^2 = 1113 kN \quad (15)$$

Since the percentage difference with $N_{comp.}$ is 6%, the result provided by SAP 2000 can be considered acceptable.

Let us consider the values of the analysis of the loads used in the SAP2000 model. However, the average seismic unit weight is $w_{mean} = 10.60$ kN/m^2, which corresponds to normal stress at the base of the column in question equal to:

$$N'_{simpl.} = n_{st} \cdot A_{trib.} \cdot w_{mean} = 6 \cdot 18.55 m^2 \cdot 10.60 kN/m^2 = 1180.23 kN \quad (16)$$

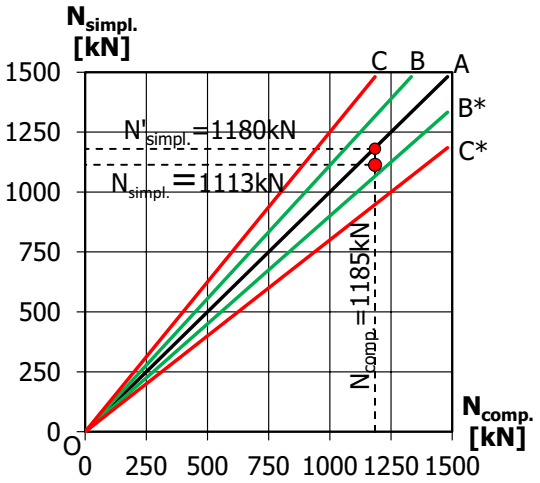

Fig. 11 Case 2: acceptability of results in terms of normal effort at the central column base

Value practically identical to that calculated by SAP2000, as highlighted in Fig. 11, with the points associated with the two comparison values of N, calculated with Eqs. (15) and (16), located near the bisector OA of the results' acceptability diagram.

4.2.2 Verification of dynamic modal analysis

Figure 12 summarizes the preliminary information obtained by SAP2000 for the first three vibration modes of case study 2. The modal modes, represented in the figure both in plan and elevation, show a first rotational mode, with period $T_{comp.,1} = 1.14$ if the percentage of effective

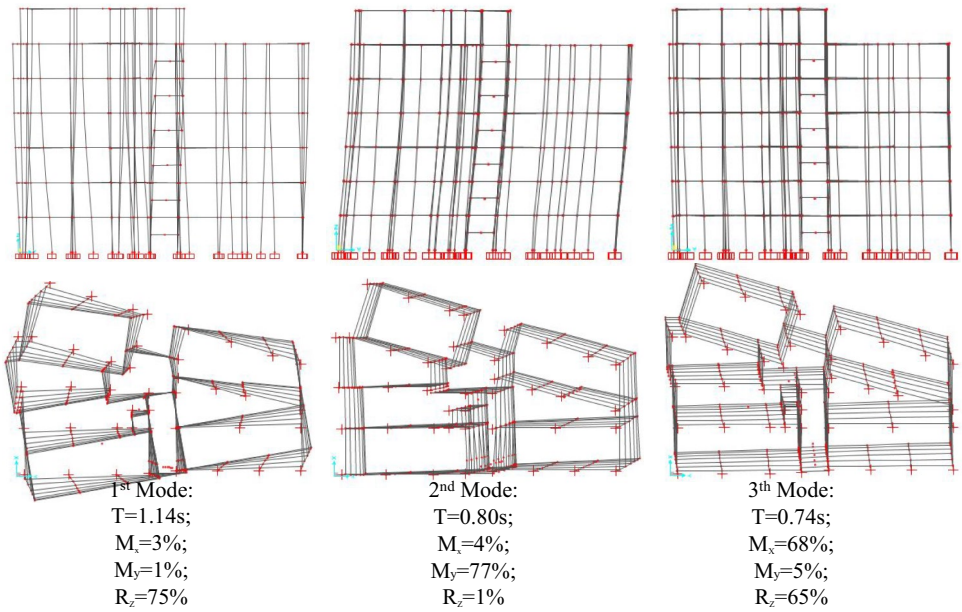

Fig. 12 Case 2: dynamic characteristics of the first three vibrating modes of the structure

rotational mass equals $R^*_{comp.,1,z} = 75\%$. The second vibration mode is substantially translating along the y-axis, with a vibration period $T_{comp.,2,y} = 0.80$ s and participant mass fraction equal to $M^*_{comp.,2,y} = 77\%$. The third mode is translating along the x-direction with rotational coupling ($R^*_{comp.,3,z} = 65\%$); the corresponding period of vibration is $T_{comp.,3,x} = 0.74$ s, while the participating mass fraction is equal to $M^*_{comp.,3,x} = 68\%$.

To check the correctness of the vibration period values, in analogy with case study #1, we can again refer to the simplified equation [7.3.6] of the NTC2018 (see Eq. (3)). Therefore, by applying horizontal forces equal to the seismic weights of the floor ($W_1 = 4652.7$ kN, $W_2 = W_3 = W_4 = W_5 = 4147.9$ kN, $W_6 = 3906.3$ kN, $W_7 = 1257.1$ kN) to the centre of gravity of the seven floors, the following displacements are obtained at SAP2000 at the top of the building: $d_x = 0.274$ m and $d_y = 0.257$ m. The corresponding simplified periods along the two main directions of the building are:

$$\text{direzione x: } d_x = 0.274\text{m} \Rightarrow T_{simpl.,x} = 2 \cdot \sqrt{d_x} = 2 \cdot \sqrt{0.274} = 1.05s$$
$$\text{direzione y: } d_y = 0.257\text{m} \Rightarrow T_{simpl.,y} = 2 \cdot \sqrt{d_y} = 2 \cdot \sqrt{0.257} = 1.01s \quad (17)$$

The comparison between the first three fundamental periods obtained from SAP2000 with the ones calculated from simplified expressions (17) is plotted in Fig. 6a. This comparison shows a difference acceptable only for the first mode (point P). For the second and third modes, the corresponding points Q and R show more than 20% differences due to the structural irregularity of case 2.

For the case in question, a comparison was made in terms of participating masses, using the same criterion illustrated and applied in §4.1.2. Therefore, assuming in both directions x and y the simplified modal of the linear type shown in Fig. 13b, normalized to the top modal displacement ($\psi_{7,1} = 1$), we have:

$$\Psi_{1x,1y} = \begin{Bmatrix} \Psi_{7,1} \\ \Psi_{6,1} \\ \Psi_{5,1} \\ \Psi_{4,1} \\ \Psi_{3,1} \\ \Psi_{2,1} \\ \Psi_{1,1} \end{Bmatrix} = \begin{Bmatrix} h_{tot}/h_{tot} \\ h_6/h_{tot} \\ h_5/h_{tot} \\ h_4/h_{tot} \\ h_3/h_{tot} \\ h_2/h_{tot} \\ h_1/h_{tot} \end{Bmatrix} = \begin{Bmatrix} 19.2/19.2 \\ 19.2/22.4 \\ 16/22.4 \\ 12.8/22.4 \\ 9.6/22.4 \\ 6.4/22.4 \\ 3.2/22.4 \end{Bmatrix} = \begin{Bmatrix} 1 \\ 0.86 \\ 0.71 \\ 0.57 \\ 0.43 \\ 0.29 \\ 0.14 \end{Bmatrix} \quad (18)$$

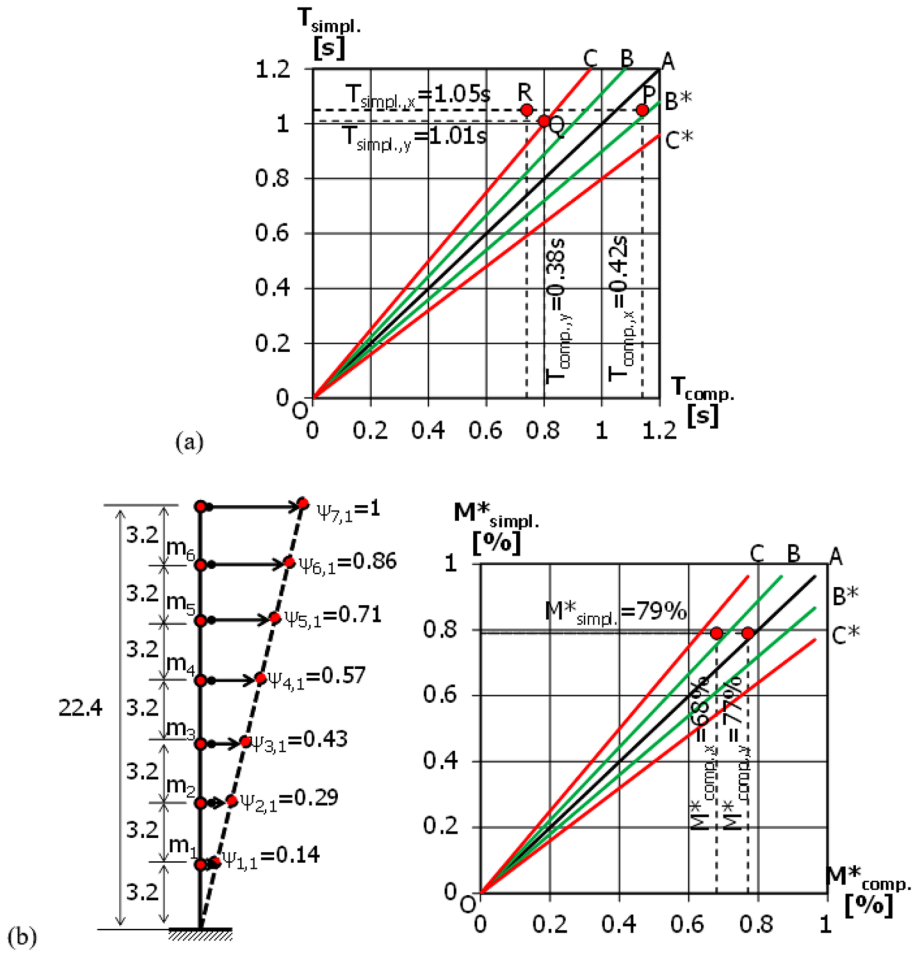

Fig. 13 Case 2: acceptability of the results in terms of their vibration periods (**a**) and participating masses (**b**)

Since the seismic masses of the seven decks are valid:

The comparison between the participating mass fractions

$$m_1 = \frac{W_1}{g} = \frac{4652.7kN}{9.81m/s^2} = 474.3\frac{kN\cdot s^2}{m}; m_2 = m_3 = m_4 = m_5 = \frac{W_{2\div5}}{g} = \frac{4147.9kN}{9.81m/s^2} = 422.8\frac{kN\cdot s^2}{m};$$
$$m_6 = \frac{W_6}{g} = \frac{3906.3kN}{9.81m/s^2} = 398.2\frac{kN\cdot s^2}{m}; m_7 = \frac{W_7}{g} = \frac{1257.1kN}{9.81m/s^2} = 128.10\frac{kN\cdot s^2}{m}; \mathrm{m_{tot}} = \sum_{j=1}^{7} m_j = 2691.80\frac{kN\cdot s^2}{m} \quad (19)$$

The corresponding simplified participant mass percentage is:

given by SAP2000 for the first two translational vibration modes ($M^*_{comp.,Y}=77\%$ and $M^*_{comp.,X}=68\%$) calculated by

$$M^*_{simpl.} = \frac{\left(\sum_{j=1}^{7} m_j\cdot\psi_{j,1}\right)^2}{m_{tot}\cdot\left(\sum_{j=1}^{7} m_j\cdot\psi^2_{j,1}\right)} \quad (20)$$
$$= \frac{(474.3\cdot0.14 + 422.8\cdot(0.29+0.43+0.57+0.71) + 398.2\cdot0.86 + 128.10\cdot1)^2}{2691.8\cdot\left(474.3\cdot0.14^2 + 422.8\cdot(0.29^2+0.43^2+0.57^2+0.71^2) + 398.2\cdot0.86^2 + 128.10\cdot1^2\right)} =$$
$$= \frac{1912057}{2691.8\cdot896.28} = 79\%$$

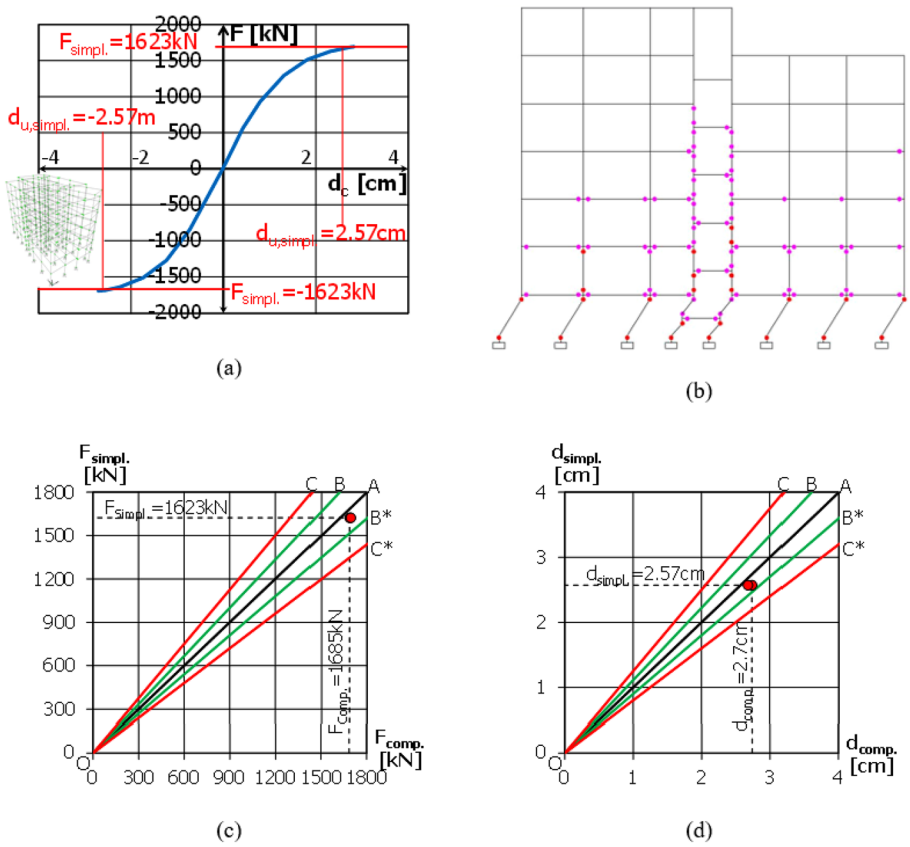

Fig. 14 Case 2: **a** pushover curves of SAP2000 and comparison with manually calculated force and displacement values; **b** collapse mechanism of the structure analyzed with SAP; **c**, **d** Acceptability of the results in terms of forces and displacements

hand with Eq. (20) is plotted in Fig. 13b. In this case, the check is satisfactory also since the point associated with the mass calculated along the y-direction is on the bisector OA, while the point indicative of the comparison of the participating masses along the x-axis is close to the limit line OB representing a deviation equal to 13.9%, which can be considered acceptable considering of the irregularity of the structure.

4.2.3 Verification of non-linear static analysis

Figure 14a illustrates the pushover curves of case study 2, obtained with SAP2000, considering the distribution of forces proportional to the seismic masses applied along the ± y-direction. For both directions of the forces' application, it is possible to observe a linear elastic behaviour up to a value of the base shear equal to about 1000 kN and then have a non-linear behaviour up to its maximum $F_{comp.} = 1685$ kN, which corresponds to an ultimate displacement $d_{u,comp.} \sim 2.7$ cm. The corresponding failure mechanism in the last analysis step with SAP2000 is illustrated in Fig. 14b. In this case, as often observed in the reconnaissance of seismic damage in reinforced concrete buildings designed for gravitational loads only, the building collapses according to the classic and undesirable soft story mechanism, characterized by the formation of plastic hinges at the top and the column base of the first story, while the remaining part of the structure, which ranges from the second to the seventh floor of the building, basically behaves like a rigid block that collapses on the first level of the building.

Similarly, to what was discussed in §4.1.3, to check the correctness of the pushover curve of Fig. 14a in terms of forces, it is still possible to apply the kinematic theorem of the limit analysis of structures (Massonet and Save, 1978) to the mechanism of the soft story of Fig. 14b. Therefore, by equating the work L_e of the external forces $F_1, F_2, \ldots, F_7$, assumed proportional to the masses, with the work of the internal forces L_i performed by the plastic moments M_{pl} of the hinges activated at the ends of the first story column in the local mechanism of Fig. 14b, we have:

$$\begin{aligned} L_i &= \sum_{i=1}^{7} F_i \cdot \delta_i \cong \left(\sum_{i=1}^{7} F_i \right) \cdot \delta_c \cong F_u \cdot (\vartheta_{pl} \cdot h_1) \\ L_e &= 2 \cdot n_c \cdot M_{c,pl} \cdot \vartheta_{pl} \\ L_i &= L_e \Rightarrow F_u = \frac{2 \cdot n_c \cdot M_{c,pl}}{h_1} \end{aligned} \tag{21}$$

where n_c is the number of first story columns where plastic hinges are activated, $M_{c,\,pl}$ (average value between all

columns), h_1 is the height of the first level, θ_{pl} is the plastic rotation of the hinges at the ends of the column.

For the examined case study, it results in $n_c = 42e$ $h_1 = 3.20$ m. Simultaneously, the average column resisting moment associated with the acting axial force is $M_{c,pl} = 61.83$ kN m. Therefore, the ultimate base shear that can support the collapsing structure according to the soft story mechanism is:

$$F_{simpl.} = \frac{2 \cdot n_c \cdot M_{c,pl}}{h_1} = \frac{2 \cdot 42 \cdot 61.83kNm}{3.2m} = 1623kN \quad (22)$$

This value is very close to the maximum base shear $F_{comp.} = 1685$ kN given by SAP2000, as shown both in the diagram of Fig. 14a and in the diagram of acceptability of the results of Fig. 14c from which it can be observed how the point of comparison between the two quantities calculated with software and by hand is close to the bisector OA, being the difference between the two comparative quantities equal to 3.7% and therefore technically acceptable [33].

For the building in consideration, the correctness of the results of the pushover analysis was also verified in terms of dc displacements of the control point of the structure, which for the capacity curve of Fig. 14a is equal to $d_c = 2.74$ cm in the + y direction $d_c = 2.68$ cm in the − y-direction. Also, in this case, it is possible to estimate the ultimate displacement of the control point d_u; Manual can still be evaluated using the Eqs. (10) to (14), being:

$$k = \frac{W_{tot}}{d} = \frac{26407.7kN}{0.257m} = 102753.70 \text{ kN/m} \quad (23)$$

the lateral elastic stiffness of the structure in the y-direction (see Eq. (17));

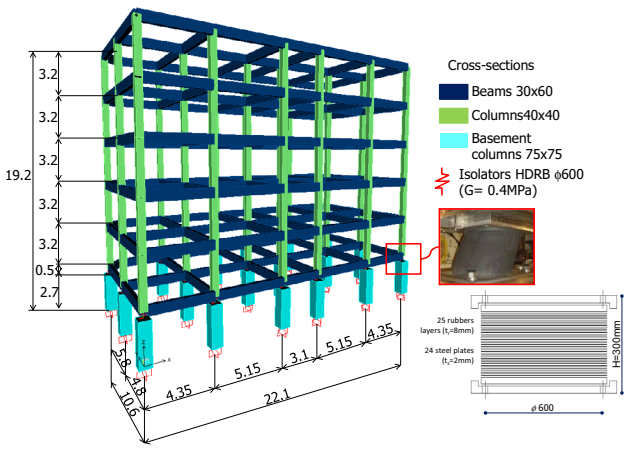

Fig. 15 Case 3: finite element model of the seismically isolated structure with 18 rubber insulators

$$d_{y,simpl.} = \frac{F_y}{k} = \frac{1000kN}{102753.7kN/m} = 0.0097m \quad (24)$$

the displacement at an elastic limit corresponding to the formation of the first hinge in the model, which, as already mentioned, is activated in correspondence with a cutting at the base equal to about 1000 kN.

Consistently with the plastic hinge model implemented in the SAP2000 model for columns with non-conforming brackets, the plastic displacement d_{pl} of the control point can be evaluated considering a rotational capacity equal to $\theta_{pl} = 1\%$ rad; therefore, we have:

$$d_{pl,simpl.} = \vartheta_{pl} \cdot h_1/2 = 0.01rad \cdot 3.2m/2 = 0.016m \quad (25)$$

In Eq. (25), the half-height of the columns was considered ($h_1/2 = 1.6$ m) to consider the reduced height of the columns of the stairwell, which in the computational analysis were the critical elements that caused the termination of the analysis.

The ultimate displacement of the control point can, therefore, be estimated as equal to:

$$d_{u,simpl.} = d_{y,simpl.} + d_{pl,simpl.} = 0.0097 + 0.016 = 0.0257m \quad (26)$$

The comparison between the values of the ultimate displacements obtained by SAP2000 and those calculated by hand with Eqs. (23) to (26) is reported in Fig. 14a and the acceptability diagram of Fig. 14d. Both figures show that the computational analysis results in the non-linear field are also acceptable in terms of displacements since the differences between the values under consideration are approximately 5%.

4.3 Case 3: six-storey seismically isolated building

As a third case study, this paragraph presents and discusses the simplified hand calculations used to check the numerical results obtained with SAP2000 for the modal analysis carried out on a structure of residential buildings in reinforced concrete, seismically isolated by 18 elastomeric isolators (Cuomo, 2004). As shown in Fig. 15, the case study in question has a rectangular plan with a surface area $A_{floor} = 315$ m^2. The building's total height is 19.20 m for six floors, with a floor height of 3.20 m. The upper six floors of the structure have 30 × 60 beams in both x and y directions, while all the columns have a 40 × 40 cross-section. The seismic isolation system is located on the first level beams' intrados, while the seismic isolators are supported by 18 basement columns (lower structure) having 75 × 75 cross-sections.

All seismic isolators are made up of HDRB elastomeric devices with a circular section of diameter $\phi = 600$ mm. The insulators' total height is 300 mm, while the total

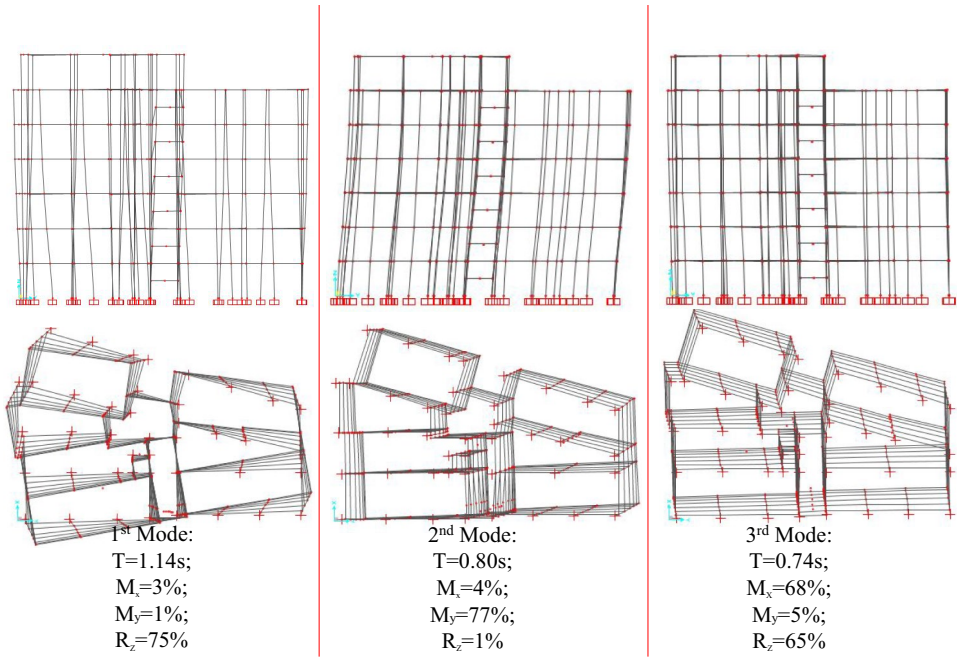

Fig. 16 Case 3: dynamic characteristics of the first three vibrating modes of the seismically isolated structure

height of the rubber layers is 200 mm. The primary and secondary shape factors are $S_1 = 20$ and $S_2 = 3$, respectively. The devices are soft rubber, with a shear modulus of G = 0.4 MPa. The equivalent horizontal stiffness of each insulator is $k_h = 570$ kN/m, and the weight of each device is 5 kN. Figure 16 summarizes the dynamic characteristics of the first three vibrating modes of the structure. The isolation system allows the decoupling of the vibration modes. The first way is a pure translation in the y-direction, with a proper period equal to $T_{comp.,Y} = 2.86$ s and participant mass fraction $M^*_{comp.,X} = 98\%$. Similarly, the second mode is a pure translation along the x-axis, with a vibration period $T_{comp.,X} = 2.84$ s and participant mass fraction $M^*_{comp.,X} = 98\%$. The third way is pure rotational, with period $T_{comp.,Z} = 1.26$ s, and participant mass fraction equals $R^*_{comp.,Z} = 95\%$.

A simple check of the results of the modal analysis can be carried out using the equation of the period of the simple oscillator (S-DOF) of mass equal to the total mass of the isolated building (m_{tot}) and, neglecting the deformability of the beams and the upper structure, of lateral stiffness equal to the equivalent horizontal stiffness of the isolation system (k_{isol}).

To this end, also assuming a seismic unit weight of the building equal to $w_i = 10\text{kN/m}^2$ ($i = 1 \div 6$), the seismic weight of the upper structure is:

$$W_{upperstruct.} = n \cdot A_{floor} \cdot w_i = 6 \cdot 315m^2 \cdot 10kN/m^2 = 18900kN \quad (27)$$

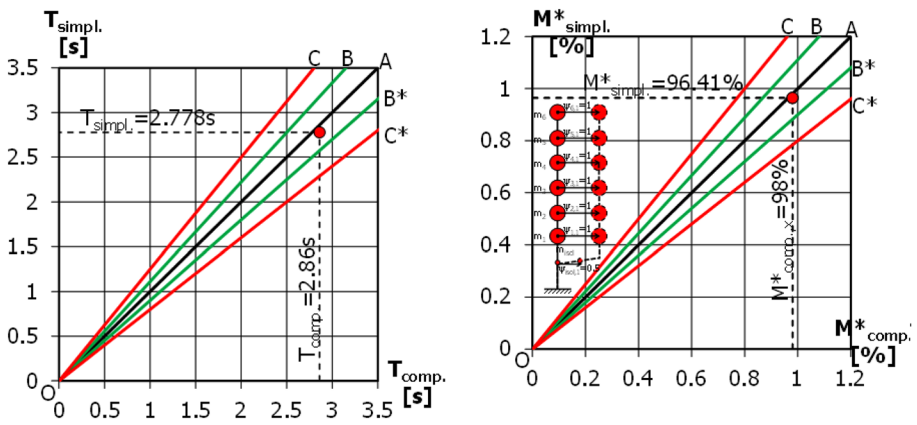

(a) (b)

Fig. 17 Case 3: acceptability of results in terms of their vibration periods (**a**) and participating masses (**b**)

The weight of the isolation system and that of the lower structure are respectively:

$$W_{isol} = n_{isol} \cdot w_{isol.} = 18 \text{ isolatori} \cdot 5kN = 90kN \tag{28}$$

$$\begin{aligned} W_{lowerstruct.} &= n_{isol} \cdot w_{basement\_column} \\ &= 18 \cdot 2.7\text{m} \cdot 0.752\ \text{m}^2 \cdot 25\text{kN/m}^3 = 683.44\text{kN} \end{aligned} \tag{29}$$

Therefore, the total weight of the product is:

$$\begin{aligned} W_{tot} &= W_{upperstruct.} + W_{isol} + W_{lowerstruct.} \\ &= 18900 + 90 + 683.44 = 19673.44\text{kN} \end{aligned} \tag{30}$$

Which corresponds to the following total mass:

$$m_{tot} = \frac{W_{tot}}{g} = \frac{19673.44kN}{9.81m/s^2} = 2005.45\frac{kN \cdot s^2}{m} \tag{31}$$

Since the equivalent horizontal stiffness of the 18 insulators is:

$$k_{isol} = n_{isol} \cdot k_h = 18 \cdot 570\text{kN/m} = 10260\text{kN/m} \tag{32}$$

The vibration period of the equivalent S-DOF system to the structure in question is:

$$T_{manuale} = 2\pi \cdot \sqrt{\frac{m_{tot}}{k_{isol}}} = 2\pi \cdot \sqrt{\frac{2005.45\frac{kN \cdot s^2}{m}}{10260\frac{kN}{m}}} = 2.778s \tag{33}$$

The comparison between the period given by SAP2000 ($T_{comp.} = 2.86$ s) and the estimated value obtained using Eq. (33) is proposed in the diagram of Fig. 17a, from which it is once again possible to ascertain the correctness of the computational calculation, having the two comparative quantities a difference of 2.9% and therefore acceptable.

In analogy to what has been illustrated for the previous cases, it is also possible to check with simple calculations the participating masses' values of the first two vibration modes in Fig. 16. If a first normalized mode of vibration is assumed along the x or y direction characterized by the modal shown in Fig. 17b, or by the following modal shifts:

$$\Psi_{1x,1y} = \begin{Bmatrix} \Psi_{6,1} \\ \Psi_{5,1} \\ \Psi_{4,1} \\ \Psi_{3,1} \\ \Psi_{2,1} \\ \Psi_{1,1} \\ \Psi_{isol,1} \\ \Psi_{baggioli,1} \end{Bmatrix} = \begin{Bmatrix} 1 \\ 1 \\ 1 \\ 1 \\ 1 \\ 1 \\ 0.5 \\ 0 \end{Bmatrix} \tag{34}$$

And since the seismic masses are worth:

$$\begin{aligned} &m_1 = m_2 = m_3 = m_4 = m_5 = m_6 = \frac{W_{upperstruct.}}{6 \cdot g} = \frac{18900kN}{6 \cdot 9.81m/s^2} = 321.10\frac{kN \cdot s^2}{m}; \\ &m_{isol} = \frac{W_{isol}}{g} = \frac{90kN}{9.81m/s^2} = 9.17\frac{kN \cdot s^2}{m}; m_{lowerstruct.} = \frac{W_{lowerstruct.}}{g} = \frac{683.44kN}{9.81m/s^2} = 69.67\frac{kN \cdot s^2}{m} \end{aligned} \tag{35}$$

The simplified participant mass percentage can be estimated with the following equation:

$$\begin{aligned} M^*_{simpl.} &= \frac{\left(\sum_j m_j \cdot \psi_{j,1}\right)^2}{m_{tot} \cdot \left(\sum_j m_j \cdot \psi^2_{j,1}\right)} \\ &= \frac{(6 \cdot 321.10 \cdot 1 + 9.17 \cdot 0.5 + 69.67 \cdot 0)^2}{2005.45 \cdot \left(6 \cdot 321.10 \cdot 1^2 + 9.17 \cdot 0.5^2 + 69.67 \cdot 0^2\right)} \\ &= \frac{3729505.09}{2005.45 \cdot 1928.90} = 96.41\% \end{aligned} \tag{36}$$

The comparison between the participating mass percentages obtained from SAP2000 for the first mode along with the two main directions of the building ($M^*_{comp.,\,X} = M^*_{comp.,\,Y} = 98\%$) and the approximate one evaluated with Eq. (36) is summarised in the acceptability diagram of Fig. 17b. This confirms modal analysis's reliability, as the graph's corresponding point is close to the bisector OA, with a difference between the values in comparison equal to 1.65%.

5 Conclusions

Modern structural engineers' design work has been greatly impacted by the increasingly rigorous limitations imposed by contemporary technical requirements, and substantial advances in information technology and computational mechanics. Examining the growth of technical research related to devices and types of equipment over the last four decades reveals this influence. Plotters have supplanted traditional drafting equipment, while slide rules have given way to commercial computation software.

Because of this dramatic shift, younger engineers believe that getting and mastering the appropriate commercial software is sufficient to become a qualified structural engineer (Ghersi, 2020) [34]. The sound of structural computation software has become analogous to that of a guitarist's guitar, with some preferring the harsh sound of a Fender and others preferring the full and resonant tones of a Gibson. When faced with the challenge of selecting the best (calculation) tool, aspiring structural designers frequently ask the critical question: "Dear engineer, I am thinking about acquiring a program; which one do you recommend?".

However, it is critical to understand that a calculating program alone does not constitute a structural engineer. Regardless of the analysis technique used, the engineer must have the essential abilities to forecast the behaviour of the structure under consideration. Structural computation software is a powerful and increasingly important tool for structural engineers, but only if the findings can be interpreted and verified.

In this sense, this article gives examples of manual calculations that can be used to check the conclusions of structural analysis tools. For Case 1, different verifications were made and the comparison in terms of periods of vibration and percentages of participating mass along the two main directions allows us to state that the FEM model provides acceptable results for linear dynamic analysis. It further shows that there are no errors in the modelling as well during the assignment of the seismic masses to the structure phases. It was also noticed that the values of forces and displacements allow tracing the suggested curve with an elastic-perfectly plastic trend, which envelops the pushover curves well to confirm the correctness of the results obtained with the software and, simultaneously, the effectiveness of the simplified methods. In Case 2 the checks were satisfactory and only a deviation equal to 13.9% was obtained, which can be considered acceptable considering of the irregularity of the structure. Furthermore, it was shown that the computational analysis results in the non-linear field are also acceptable in terms of displacements since the differences between the values under consideration are approximately 5%. Finally for the last Case 3 the comparison between the participating mass percentages obtained from SAP2000 for the first mode along with the two main directions of the building was made and confirms modal analysis's reliability, as the graph's corresponding point is close to the bisector OA, with a difference between the values in comparison equal to 1.65%. These examples show how simple and quick computations can be used to assess the acceptability and dependability of the software's numerical results, as specified by NTC2018 10.2.1.

Authors contributions GB main concepts, data collections, literature review, data analysis, drafting, initial draft, reviewing, analyzing, final drafting. MTN data collections, literature review, drafting, initial draft, reviewing, analyzing, final drafting.

Funding There is no funding sponsor for this work.

Data availability The data used to support the findings of this study are included in the article.

Declarations

Conflict of interest The authors declare that there is no conflict of interest regarding the publication of this paper.

Authors agreement The author agrees to grant the publisher an exclusive license to publish the paper. The author represents and warrants that the paper is original has not been published previously.

References

1. I. M. of I. and NTC (2018) Norme Tecniche per le Costruzioni. DM 17/1/2018. Gazz. Uff. della Repubb. Ital.
2. Ministero delle Infrastrutture (2008) NTC 2008- norme tecniche per le costruzioni. Decreto Minist.
3. Pacella G, Sandoli A, Calderoni B, Brandonisio G (2022) Open issues on non-linear modelling for seismic assessment of existing masonry buildings. Proc Struct Integr. https://doi.org/10.1016/j.prostr.2023.01.170
4. Sandoli A, Pacella G, Calderoni B, Brandonisio G, Lignola GP, Prota A (2022) Seismic fragility assessment of Balvano (Potenza, Italy) pre and post 1980 Irpinia's earthquake. Proc Struct Integr. https://doi.org/10.1016/j.prostr.2023.01.171
5. Waheeb SA (2023) Environmental and cultural sustainability of the architectural elements of two historical mosques in historic Jeddah. J Umm Al-Qura Univ Eng Archit. https://doi.org/10.1007/s43995-022-00011-z
6. Ruggieri S, Uva G (2020) Accounting for the spatial variability of seismic motion in the pushover analysis of regular and irregular rc buildings in the new italian building code. Buildings. https://doi.org/10.3390/buildings10100177
7. Lourenço PB (1996) Computational strategies for masonry structures [Ph.D thesis]
8. Naqash MT, Farooq QU (2018) Performance of rigid steel frames under adequate soil conditions using seismic code provisions. Open J Civ Eng. https://doi.org/10.4236/ojce.2018.82008
9. Sorrentino P, Brandonisio G, De Luca A (2022) Complex monumental buildings. Definition of complexities and structural

implications. Proc Struct Integr. https://doi.org/10.1016/j.prostr.2023.01.213
10. Umar M, Shah SAA, Shahzada K, Naqash T, Ali W (2020) Assessment of seismic capacity for reinforced concrete frames with perforated unreinforced brick masonry infill wall. Civ Eng J. https://doi.org/10.28991/cej-2020-03091625
11. Tayyab M, Ayed N, Alluqmani E, Umar Q (2023) A comparative analysis of design and analysis methods for steel connections: contrasting American and European perspectives. J Umm Al-Qura Univ Eng Archit. https://doi.org/10.1007/s43995-023-00037-x
12. Hill R (1954) History of strength of materials. J Mech Phys Solids. https://doi.org/10.1016/0022-5096(54)90010-1
13. Raphael R (2016) Galileo's two new sciences as a model of reading practice. J Hist Ideas. https://doi.org/10.1353/jhi.2016.0029
14. Drake S, Schouls PA (1969) Galileo: two new sciences. Renaiss. Reform. https://doi.org/10.33137/rr.v11i2.13685
15. (1978) Galileo, two new sciences. Hist Math. https://doi.org/10.1016/0315-0860(78)90153-2
16. Befalazott Tartókkal K, Kazinczy G (1914) Experiments with clamped endbeams, pp 101–104
17. Baker J, Heyman J (1969) Plastic design of frames. https://doi.org/10.1017/cbo9780511586514
18. Onat ET, Prager W (1953) Limit analysis of arches. J Mech Phys Solids. https://doi.org/10.1016/0022-5096(53)90012-X
19. (1952) Limit analysis of voussoir (segmental) and concrete archs. ACI J Proc. https://doi.org/10.14359/11822
20. Heyman J (1966) The stone skeleton. Int J Solids Struct. https://doi.org/10.1016/0020-7683(66)90018-7
21. Brandonisio G, Naqash MT, Farsangi EN (2022) Seismic performance assessment of the historical Reggio Calabria cathedral. Open Civ Eng J. https://doi.org/10.2174/18741495-v16-e2209291
22. Kallioras S, Graziotti F, Penna A, Magenes G (2022) Effects of vertical ground motions on the dynamic response of URM structures: comparative shake-table tests. Earthq Eng Struct Dyn. https://doi.org/10.1002/eqe.3569
23. Wang H, Jia M, Yao Y, Chen X, Zhang Z (2023) Influence of the vertical component of Yangbi ground motion on the dynamic response of RC frame and brick-concrete structure. Buildings. https://doi.org/10.3390/buildings13010147
24. Wilson EL, Der Kiureghian A, Bayo EP (1981) A replacement for the srss method in seismic analysis. Earthq Eng Struct Dyn. https://doi.org/10.1002/eqe.4290090207
25. Wilson CR (2015) Termination of the response spectrum method, July 13, History of the RSM for seismic analysis the equation which that should have terminated the RSM of analysis M2(t) Ct, vol 3
26. Kreslin M, Fajfar P (2011) The extended N2 method taking into account higher mode effects in elevation. Earthq Eng Struct Dyn. https://doi.org/10.1002/eqe.1104
27. Fajfar P, Dolšek M (2012) A practice-oriented estimation of the failure probability of building structures. Earthq Eng Struct Dyn. https://doi.org/10.1002/eqe.1143
28. Structural Software for Analysis and Design | SAP2000. https://www.csiamerica.com/products/sap2000. Accessed 21 Nov 2020
29. Marrazzo A (2020) Seismic adaptation of a reinforced concrete building designed for vertical loads only: from simplified and advanced structural analysis to the design of the temporary works necessary for the execution of the cutting of some columns. University of Naples Federico II [in Italian]
30. P M (1969) Theory of buildings vol 2—buildings in reinforced concrete. Liguori Editore **(in Italian)**
31. Massonnet C, Save M (1976) Structures à un Paramètre, 3e édition, Liège. Nelissen B (ed) Italian translation: Calcolo Plastico a Rottura delle Costruzioni, p 704, 1980. CLUP (Coop. Libraria univ. del politecnico di Milano), p 637
32. Scipione S (2017) Seismic capacity of an existing reinforced concrete building designed for vertical loads only **(in Italian)**
33. Naqash T (2020) Pushover response of multi degree of freedom steel frames. Civ Eng J. https://doi.org/10.28991/cej-2020-SP(EMCE)-08
34. Ghersi A (2020) Let's play… 'I design the building' A new video game allows you to become structural engineers. Lo Strutturista, n. 2 **(in Italian)**